

Molecular Dynamics and Quantum Chemical Calculation for 3,4-Dihydropyrimidin-2(1H)-Ones As Corrosion Inhibitors of Mild Steel in 1M Hydrochloric Acid Solution

Jian Li^{1,2,*}, Xueli Xu¹, Kai Shi¹, Yong Zhou¹, Xian Luo² and Yue Wu¹

¹ School of Materials Science and Engineering, Xi'an Shiyou University, Xi'an 710065, PR China

² School of Materials, Northwestern Polytechnical University, Xi'an 710072, PR China

*E-mail: jeeanlee@163.com

Received: 17 August 2012 / Accepted: 17 September 2012 / Published: 1 October 2012

Molecular dynamics (MD) simulations and quantum chemical calculations were used to study the adsorption and the corrosion inhibition of three 3,4-dihydropyrimidin-2(1H)-ones (DHPM-1~3) on Fe(0 0 1) surface in pure water and 1 M hydrochloric acid solution. The MD simulation results indicate the three molecules are inclined to adsorbed on the Fe(0 0 1) surface, and the heterocyclic rings of the molecules are parallel to the Fe surface, while the benzene rings of three molecules point out to the aqueous side. Among the three inhibitor molecules, 5-acetyl-6-methyl-4-(3-nitro phenyl)-3,4-dihydropyrimidin-2(1H)-one (DHPM-2) has the highest binding energy, the largest deformation energy, the largest coverage effect of single molecule, and consequentially the largest adsorption inclination on Fe(0 0 1) substrate, furthermore, the molecule has larger binding energy in 1M HCl solution than in pure water, its combination with Fe surface is mainly the contribution from the VanderWals energy; the quantum calculations demonstrate that DHPM-2 has the lower E_{LUMO} , the smaller energy gap ΔE , and the largest dipole moment μ , which suggest it will interact with Fe atoms more actively. All of these imply that the better inhibition efficiency of DHPM-2 can be anticipated among these three molecules.

Keywords: Mild steel, corrosion inhibitor, dihydropyrimidin-ones, molecular dynamics, quantum chemical calculations

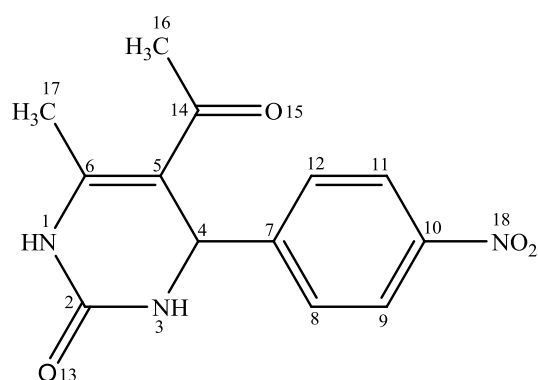
1. INTRODUCTION

The application of inhibitors to control the corrosion of different metal materials is very common in various industries. It is known that organic compounds, especially those with N, S, O and aromatic rings, have significant inhibition efficiency. For the purpose to maximize or optimize the effect of corrosion inhibition, large numbers of organic compounds were studied [1-6]. Due to the

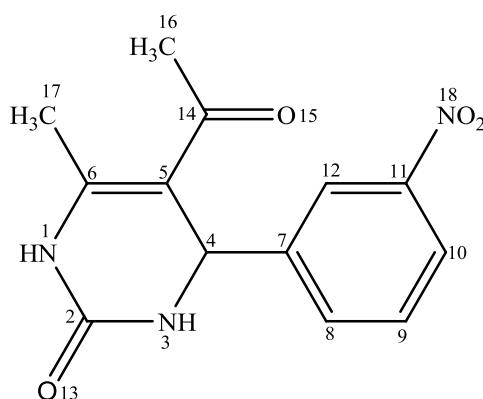
experimental study usually consumes much time and money, molecular dynamics (MD) simulation and quantum chemical calculation become common methods to investigate the mechanism and efficiency of the novel corrosion inhibitors [7-17].

The by-product or rejected product of pharmacy plant usually contains lots organic compounds with N, S, O atoms and aromatic rings, so they are promising to be used as an environmentally acceptable, readily available and renewable source of inhibitors. The dihydropyrimidin-one and its derivatives are widely used in the pharmaceutical industry as calcium channel blockers [18], antibiotics [19], and antihypertensive agents [20].

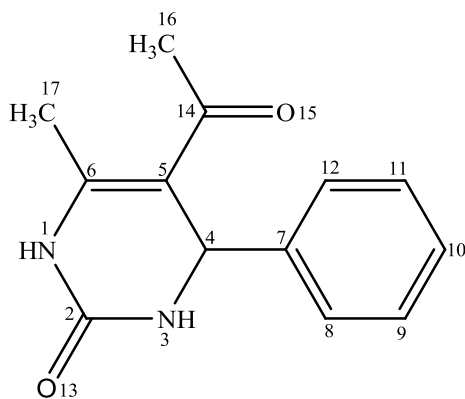
For the atomistic insight into the inhibitive adsorption and mechanism of three 3,4-dihydropyrimidin-2(1H)-ones (DHPMs) for the corrosion of mild steel in 1 M HCl solution at 25 °C, the paper gives a theoretical interpretation of three dihydropyrimidin-ones as inhibitors on Fe(0 0 1) surface by Molecular Dynamics (MD) and quantum chemical calculations. These compounds include 5-acetyl-6-methyl-4-(4-nitro phenyl)-3,4-dihydropyrimidin-2(1H)-one (DHPM-1), 5-acetyl-6-methyl-4-(3-nitro phenyl)-3,4-dihydropyrimidin-2(1H)-one (DHPM-2), and 5-acetyl-6-methyl-4-phenyl-3,4-dihydropyrimidin-2(1H)-one (DHPM-3), which are shown in Figure 1. The reasons to choose these molecules are not only because they are plenty in the waste of pharmacy plant, either they can be easily synthesized from relatively cheap materials [21-24], but more important for that the previous studies [25-30] have proved pyrimidine derivatives can act as effective steel inhibitors in acid solution, and they have high solubility in water.



(a) 5-acetyl-6-methyl-4-(4-nitro phenyl)-3,4-dihydropyrimidin-2(1H)-one (DHPM-1)



(b) 5-acetyl-6-methyl-4-(3-nitro phenyl)-3,4-dihydropyrimidin-2(1H)-one (DHPM-2)



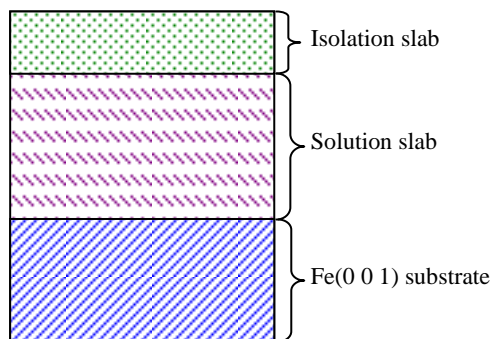
(c) 5-acetyl-6-methyl-4-phenyl-3,4-dihydropyrimidin-2(1H)-one (DHPM-3)

Figure 1. Chemical structure and IUPAC name of 3,4-dihydropyrimidin-2(1H)-ones (DHPMs).

2. SIMULATION DETAILS

Molecular dynamics (MD) simulations of the interaction between inhibitor molecules and Fe(0 0 1) in 1M HCl solution were performed using DISCOVER program with COMPASS force field [31] in Materials Studio Package from Accelrys Inc. Inhibition mechanism of three DHPMs was discussed by computing binding energies, deformation energy and equilibrium atomic configurations of different systems.

The body-centred cubic (IM-3M space group) Fe unit cell was optimized (lattice constant: $a = 2.86 \text{ \AA}$), then it was cleaved to create Fe(0 0 1) surface with 11 atom layers in thickness. The molecules were optimized respectively before they were used to construct solution slab and isolation slab. The interface supercell was built by sequentially stacking the solution slab and isolation slab on Fe(0 0 1) substrate (Figure 2), the role of isolation slab is a separation between the solution slab and Fe(0 0 1) substrate to avoid their interaction.

**Figure 2.** Schematic of interface supercell

The interface supercell contained 1 DHPM, 1500 H_2O , 28 H_3O^+ , 28 Cl^- , and 1331 Fe atoms. The concentration of inhibitor and HCl were about 0.035 M and 1 M, respectively. The cut off

distance, spline width and buffer width were set as 15.5 Å, 5.0 Å and 2.0 Å, respectively. The interface system was optimized as the first step, then MD simulation was performed as NVT ensemble with Anderson thermostat at 298 K, time step was set as 1fs, and 1000ps simulation time in total. In this paper, the absorptions in vacuum and pure water were also simulated and treated as the comparisons with the hydrochloric acid solution.

In order to further clarify the absorption mechanism of the selected inhibitor molecules, the quantum chemical calculations were performed using GAUSSIAN program with density function theory (DFT) method, B3LYP correlation functional, and 6-31G* (d, p) electron basis set for all atoms. The molecule geometry was optimized, and the quantum chemical parameters were calculated.

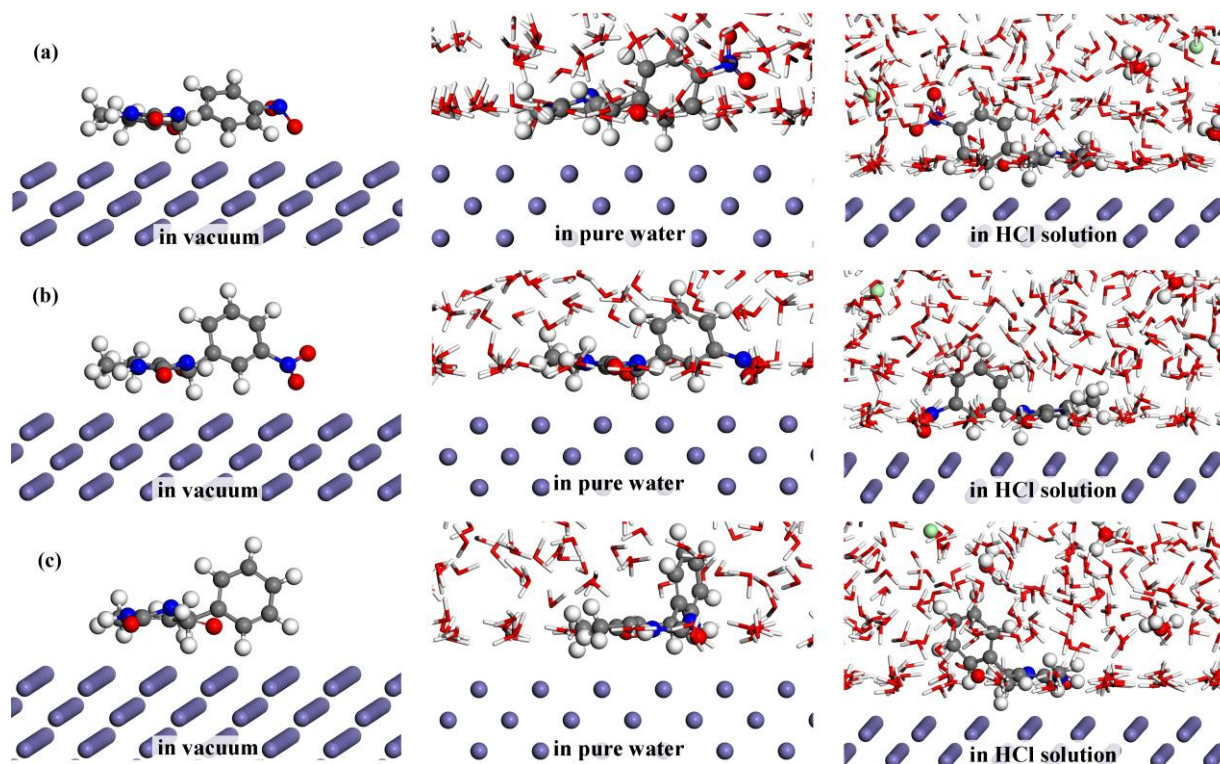


Figure 3. Equilibrium configuration of (a) DHPM-1, (b)DHPM-2, and (c) DHPM-3 absorption on Fe(0 0 1) surface.

3. RESULTS AND DISCUSSION

3.1. Equilibrium configurations of MD simulation

It is crucial that the MD simulation time should be enough to assure the interface system reaching equilibrium, and it is usually ascertained by the equilibrium criterions of temperature and energy simultaneously, i.e., the fluctuations of temperature and energy should be confined as small as possible. Taking DHPM-3 in HCl solution as an example, during the last 100 ps, the temperature

fluctuates in a range of (298 ± 16) K and the fluctuation of energy is less than 2%, indicating that the system has reached an equilibrium state.

The equilibrium configurations of three DHPMs adsorbed on Fe(0 0 1) in vacuum, pure water, and HCl solution are shown in Figure 3, respectively. It shows that the heterocyclic rings of all three molecules are nearly parallel to the Fe(0 0 1) surface, and the hetero-atoms (nitrogen and oxygen atoms) in heterocyclic ring and nitro base group are more preferred to act as main adsorption centres, a reasonable explanation is that the presence of unoccupied d-orbital of Fe exhibits an electro-positive inclination to obtain electrons from absorbed molecules [11, 32-34], therefore, when the systems reaching equilibrium, the electrons of the hetero-atoms, especially O and N atoms, are more likely absorbed by Fe atoms. The distance between Fe surface and the active atoms of molecules are listed in Table 1. The values of these distance, and including the other parameters listed in the following part of this paper, are all statistical averages over the last 100 ps of MD simulations.

Table 1. The equilibrium distance between Fe surface and the active atoms of three inhibitors in various medium.

Inhibitor	Medium	Distance (Å)						
		N1	N3	N18	O13	O15	O19	O20
DHPM-1	Vacuum	2.99	3.21	3.19	2.75	2.36	2.40	3.05
	Pure water	2.78	3.16	6.18	2.50	2.72	5.68	7.27
	HCl solution	2.79	3.18	5.26	2.64	2.63	4.58	6.45
DHPM-2	Vacuum	2.95	3.12	2.85	2.74	2.63	2.46	2.27
	Pure water	3.01	3.21	2.93	2.55	2.40	2.39	2.20
	HCl solution	2.90	3.15	2.93	2.69	2.50	2.49	2.29
DHPM-3	Vacuum	2.82	3.12	-	2.75	2.58	-	-
	Pure water	2.75	3.14	-	2.51	2.74	-	-
	HCl solution	2.75	3.14	-	2.58	2.69	-	-

Note: N1, N3 are nitrogen atoms in heterocyclic ring, N18 is the nitrogen atom in nitro group; O13 is the oxygen atom double bonded with C2, O15 is the oxygen atom in acetyl group, and O19 and O20 are the two oxygen atoms in nitro group.

It is easy to see that although the benzene rings of three molecules deviate from Fe surface, while the angles between Fe surface and the benzene rings are different in various medium: (1) in vacuum, the benzene ring of DHPM-3 is vertical to the Fe surface, otherwise, it is nearly parallel to the surface for DHPM-1, and a mediate state between the both for DHPM-2; (2) in pure water and HCl solution, the angles from Fe surface to the benzene rings of DHPM-1 and DHPM-3 are nearly equal, and they are larger than the one of DHPM-2. Besides these, the equilibrium configuration of DHPM-1 in vacuum is thoroughly different with the ones in pure water and HCl solution, the nitro base group of DHPM-1 is adhered on the Fe surface in vacuum, but in pure water and HCl solution, the nitro base group point out to the solution. That is say that the water molecules have direct effect on the supercell's equilibrium configurations, and the effect is too significant to be neglected, thus, the

simulations in vacuum are less accurate, and those simulations in vacuum should be treated as references only. Therefore, the following part of this paper will mainly discuss the MD simulations in pure water and HCl solution.

In pure water and HCl solution, the nitro base groups of DHPM-1 and DHPM-2 have different shapes, the nitro base of DHPM-2 is closely adhered on the Fe surface, while the nitro base of DHPM-1 points to the solution. It implies that the site of the nitro base group has a crucial impact on the adsorption behaviour.

Furthermore, in pure water and HCl solution, the angles between Fe surface and the benzene rings of DHPM-1 and DHPM-3 are larger than DHPM-2. Considering the parallel benzene ring is helpful to increase the molecule's coverage, it is reasonable to conclude that DHPM-2 has the best coverage effect among the three molecules, and due to DHPM-1 has an extra nitro base group comparing with DHPM-3, the coverage effect of DHPM-1 should be larger than DHPM-3, summarily, the three DHPMs have an coverage effect sequenced as DHPM-2>DHPM-1>DHPM-3. Since the coverage effect plays a positive role on the inhibition efficiency, it is reasonable to believe that DHPM-2 has the possibility to achieve the highest inhibition efficiency, and subsequently following with DHPM-1 and DHPM-3.

3.2. Binding energy of corrosion inhibitors on Fe surface

The interaction energy (E_{int}) between the surface and inhibitor molecule can be calculated as follows [7, 35-37]:

$$E_{\text{int}} = E_{\text{total}} - (E_{\text{surface}} + E_{\text{DHPM}}), \quad (1)$$

where E_{total} is the energy of the whole system (namely the surface together with the adsorbed DHPM molecule), E_{surface} and E_{DHPM} are single point energy of the surface and DHPM molecule, respectively. Binding energy (E_{bind}) is defined as the negative value of E_{int} , i.e., $E_{\text{bind}} = -E_{\text{int}}$ [7, 10, 36, 37]. Obviously, a smaller E_{int} , or a larger E_{bind} , indicates a stronger interaction between the Fe surface and the corrosion inhibitor, and the corrosion inhibitor will combine with the Fe surface more easily and tightly, so the higher inhibitive performance will be possible. The binding energies and the interaction energies of three molecules are listed in Table 2, the results of simulations in vacuum are also listed here as reference. First, all interaction energies in Table 2 are negative, showing that the combination processes of these corrosion inhibitors with Fe surface are exothermic [10, 37]. Second, the E_{bind} (namely, the negative E_{int}) values of three molecules in pure water and HCl solution are significantly larger than that in vacuum, this is because hydrogen bond interaction exists among Fe, inhibitor, and water molecules [35, 38-40], the influence of solvent effect on the interaction between inhibitors and Fe is positive and quite large, and cannot be neglected. This also exactly explains the reason of aforementioned difference between the final configurations in vacuum and in aqueous medium.

Table 2. Interaction energy (E_{int}) and binding energy (E_{bind}) of different inhibitor molecules in the various medium.

Inhibitor Molecule	E_{int} (kJ·mol ⁻¹)			E_{bind} (kJ·mol ⁻¹)		
	In vacuum	In pure water	In HCl solution	In vacuum	In pure water	In HCl solution
DHPM-1	-582.99	-644.35	-655.14	582.99	644.35	655.14
DHPM-2	-572.91	-731.29	-743.14	572.91	731.29	743.14
DHPM-3	-480.89	-622.97	-620.40	480.89	622.97	620.40

Third, the E_{bind} (or E_{int}) values of same molecule in pure water and HCl solution are nearly equal, that is say the presence of ions, namely Cl^- and H_3O^+ , have little effect on the adsorption of these molecules. Furthermore, the E_{bind} values of these molecules in the same medium are thoroughly different, the E_{bind} of DHPM-2 is the highest, and the E_{bind} of DHPM-3 is the lowest, that indicates the presence and the location of nitro base has a significant influence to the molecule's adsorption, nitro base group will interact with the ions and strengthen the inhibitor molecules absorption, and the meta-position nitro base group will have the strongest interaction.

So, by comparing the E_{bind} of three inhibitors with Fe(0 0 1) surface in pure water and HCl solution, the summary is that, the combination of DHPM-2 with Fe is firmer than DHPM-1 and DHPM-3, the likely and reasonable sequence of them is DHPM-2>DHPM-1>DHPM-3, and meta-position nitro group has more positive effect to the firmer combination. Therefore, it can be theoretically deduced that the inhibition efficiency of these three DHPMs should also have a similar sequence, namely that DHPM-2 has the highest inhibition efficiency, and DHPM-3 has the lowest among the three molecules.

3.3. Deformation of corrosion inhibitor on Fe(0 0 1) surface

The deformation degree of absorbed molecule can be evaluated by deformation energy (E_{deform}) [10, 41]:

$$E_{\text{deform}} = E_{\text{bonded molecule}} - E_{\text{free molecule}}, \quad (2)$$

where $E_{\text{bonded molecule}}$ and $E_{\text{free molecule}}$ are energies of single inhibitor molecule in adsorbed and free states, respectively. Furthermore, for the deeper insight of the molecule's interaction with the surrounding medium and Fe surface, the energy differences (ΔE) were calculated according the below formula [10]:

$$\Delta E = E_{\text{without molecule}} - E_{\text{with molecule}}, \quad (3)$$

where $\Delta E_{\text{with molecule}}$ is the energy of whole system with inhibitor molecule inside, and $E_{\text{without molecule}}$ is the energy of the system in which the inhibitor molecule has been removed. The differences

of potential energy ($\Delta E_{\text{potential}}$), non-bond energy ($\Delta E_{\text{non-bond}}$), VanderWals energy (ΔE_{vdw}) and electrostatic energy ($\Delta E_{\text{Coulomb}}$) were examined respectively.

Table 3. Deformation energy (E_{deform}) and energy differences of three inhibitor molecules in pure water and 1M HCl solution.

Inhibitor molecule	Medium	E_{deform} (kJ·mol ⁻¹)	$\Delta E_{\text{potential}}$ (kJ·mol ⁻¹)	$\Delta E_{\text{non-bond}}$ (kJ·mol ⁻¹)	ΔE_{vdw} (kJ·mol ⁻¹)	$\Delta E_{\text{Coulomb}}$ (kJ·mol ⁻¹)
DHPM-1	Pure water	119.95	1081.48	952.06	441.79	510.27
	HCl solution	119.94	1098.23	967.75	474.52	493.23
DHPM-2	Pure water	143.19	1160.37	1054.93	546.60	508.33
	HCl solution	140.32	1154.25	1048.38	547.47	500.91
DHPM-3	Pure water	114.39	1066.06	968.53	427.66	540.87
	HCl solution	113.20	1073.81	976.45	440.50	535.95

From the Table 3, one can find that all the obtained deformation energies of three inhibitors in pure water and HCl solution are above 100 kJ/mol, indicating that these absorbed molecules have deformed seriously, and DHPM-2 and DHPM-3 have the largest and smallest deformation energy respectively, thus, their deformation degree sequence should be DHPM-2>DHPM-1>DHPM-3. It is accordance with the spatial configuration of three molecules in aqueous medium (shown in Figure 2), in which the nitro base group of DHPM-2 is adhered on the Fe surface, while the nitro base group of DHPM-1 does point to the solution.

The energy differences shown in Table 3 indicate that the potential energy difference ($\Delta E_{\text{potential}}$) is mainly contributed by the non-bond energy difference ($\Delta E_{\text{non-bond}}$). The $\Delta E_{\text{non-bond}}$ comprises two parts, namely the VanderWals energy difference (ΔE_{vdw}) and electrostatic energy difference ($\Delta E_{\text{Coulomb}}$). It is found that the deformation energy (E_{deform}) of every molecule is significantly less than its $\Delta E_{\text{potential}}$, and for different molecules in the same medium, the sequence of E_{deform} is same as $\Delta E_{\text{potential}}$ and ΔE_{vdw} , when the E_{deform} is larger, the $\Delta E_{\text{potential}}$ and ΔE_{vdw} are larger too, this means that, if the ΔE_{vdw} is larger, then the VanderWals interaction between corrosion inhibitor and Fe (0 0 1) surface will be stronger, and the combination of them will be tighter and firmer. On the other hand, although the sequence of $\Delta E_{\text{non-bond}}$ and $\Delta E_{\text{Coulomb}}$ are different with the sequence of E_{deform} , however, the values of $\Delta E_{\text{non-bond}}$ and $\Delta E_{\text{Coulomb}}$ are all positive, the non-bond energy and electrostatic energy have contributions to the absorbing combination. Summarily, the VanderWals and Coulomb interactions are the dominant factors for the three inhibitors absorption and the contribution from VanderWals interaction is greater than that from Coulomb interaction.

3.4. Molecular orbital energy and dipole moment

The quantum chemical parameters, such as highest occupied molecular orbital energy (E_{HOMO}) and lowest unoccupied molecular orbital energy (E_{LUMO}), energy gap ($\Delta E = E_{\text{LUMO}} - E_{\text{HOMO}}$), dipole moment (μ), Mulliken charge on active atoms, and total energy (E_{total}) were calculated by using

GAUSSIAN program with density function theory (DFT) method. The frontier molecular orbital density distributions of three DHPMs are presented in Figure 4 a–c, and the calculation results are listed in Table 4.

Table 4. Quantum chemical calculation results of DHPMs

Molecules	E_{HOMO} (Hartree)	E_{LUMO} (Hartree)	ΔE (Hartree)	μ (Debye)	Charges on N1 / N3 / N18 / O13 / O15 / O19 / O20 (e)	E_{total} (Hartree)
DHPM-1	-0.24424	-0.08579	0.15845	6.9018	-0.59 / -0.53 / +0.38 / -0.52 / -0.49 / -0.40 / -0.40	-968.3100
DHPM-2	-0.24206	-0.08358	0.15848	6.1353	-0.59 / -0.53 / +0.39 / -0.52 / -0.48 / -0.40 / -0.40	-968.3089
DHPM-3	-0.22875	-0.05204	0.17671	3.6801	-0.59 / -0.53 / none / -0.53 / -0.49 / none / none	-763.8091

Note: N1, N3 are nitrogen atoms in heterocyclic ring, N18 is the nitrogen atom in nitro group; O13 is the oxygen atom double bonded with C2, O15 is the oxygen atom in acetyl group, and O19 and O20 are the two oxygen atoms in nitro group.

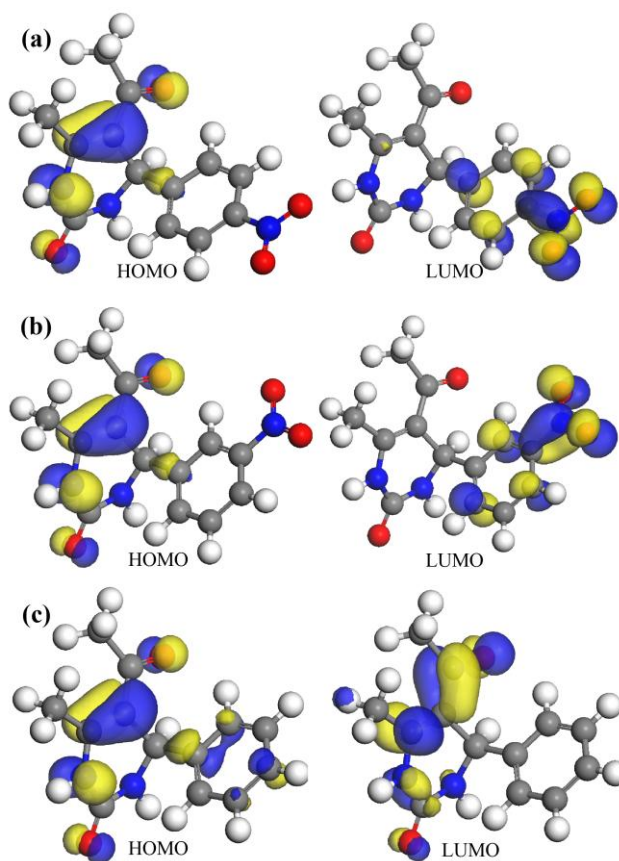


Figure 4. The frontier molecular orbital density distribution of three molecules: (a)DHPM-1, (b)DHPM-2, and (c) DHPM-3 (Isovalue=0.05)

The frontier molecular orbital (FMO) theory is often used to predict the adsorption centers of the inhibitor molecules which producing the main interaction with metal surface atoms [8, 32-34, 42-45]. According to the frontier molecular orbital theory, the formation of a transition state is due to an interaction between the frontier orbital (HOMO and LUMO) of reactants. It is known that the HOMO is the orbital that could act as an electron donor and the LUMO is the orbital that could act as the electron acceptor [34]. The widely accepted concept about inhibitor's adsorption mechanism is that: the higher HOMO energy, the greater tendency of offering electrons to metal surface atoms, and the higher inhibition efficiency; and similarly, the lower LUMO energy, the greater tendency of accepting electrons from metal surface atoms, and the better inhibition efficiency [32, 33]. The FMO theory also gives an explanation of energy gap ($\Delta E = E_{\text{LUMO}} - E_{\text{HOMO}}$) that it is an important index to characterize the molecule's stability in chemical reactions, a decrease of the energy gap usually leads to easier polarization of the molecule, and that is the basis which the concept of "activation hardness" has been defined on [8, 34, 46]. It is widely accepted that smaller energy gap ΔE means the better inhibition efficiency because the energy to remove an electron from the last occupied orbital will be low [47]. As for the dipole moment, increasing its value will facilitate the adsorption, and consequentially increase its corrosion inhibition [48, 49]. Besides these, the influences of atomic charge, total energy and the inhibition efficiency were also reported [34, 49, 50].

Figure 4 shows the HOMO orbital mainly locate at the heterocyclic ring of all three DHPMs, and considering this along with the Mulliken charges of hetero-atoms in Table 4, it is convinced that the nitrogen atoms N1, N3 and all oxygen atoms play positive roles in the adsorption process, the heterocyclic ring and the nitro group are main active centres for the adsorbing interaction, and that exactly explains why heterocyclic ring is nearly parallel to the Fe(0 0 1) surface, but benzene ring is point to the aqueous solution side. Due to the adsorption effect of nitro groups of DHPM-2 and DHPM-1, the equilibrium angles between Fe surface and their benzene rings are smaller than DHPM-3. Furthermore, due to the nitro group of DHPM-1 locates at the opposite side of benzene ring, and the inhibitor molecule stands with the VanderWals and electrostatic interactions from neighbouring water molecules or ions, therefore, the nitro group of DHPM-1 is more likely pointing out to the aqueous side, rather than adsorbing on Fe surface as the same of DHPM-2. Consequentially, for the three molecules, the angle between the benzene ring to Fe surface can be sequenced as DHPM-3 > DHPM-1 > DHPM-2, and it is consistent with the above MD simulations.

Although the E_{HOMO} decreases from DHPM-3 to DHPM-1, this means the electron donating ability of the three molecules decreases in the same order, which seems contradictory to the above MD simulation conclusion that DHPM-2 and DHPM-1 have better inhibition effect than DHPM-3, however, the decreasing E_{LUMO} and ΔE from DHPM-3 to DHPM-1 indicates the electron accepting ability and "activation hardness" are decreasing as the same order, that is consistent with the above MD conclusion. Moreover, one can find that the ΔE of DHPM-2 and DHPM-1 are very close, and the dipole moment of three molecules are $\mu_{\text{DHPM-2}} > \mu_{\text{DHPM-1}} > \mu_{\text{DHPM-3}}$. The ΔE and μ usually characterize the molecule's polarity, activation hardness. The molecule with larger ΔE and smaller μ usually has larger activation hardness. So, in a summary, although the electron donating ability of DHPM-3 is the strongest, however, the ΔE and μ indicate that DHPM-3 has the strongest resistance to the adsorption, thus, it is reasonable to conclude that DHPM-3 has less adsorption inclination and inhibition efficiency

than DHPM-2 and DHPM-1. Otherwise, due to DHPM-2 has the smaller energy gap ΔE , the highest dipole moment, and negative E_{HOMO} , all of these suggests DHPM-2 is more likely to achieve the best inhibition efficiency than the other two organics.

4. CONCLUSIONS

The molecular dynamics (MD) simulation results show that three DHPM molecules can adsorb on the iron surface through the nitrogen atoms N1, N3 and the oxygen atoms with the benzene ring towards the aqueous solution, and the -acetyl-6-methyl-4-(3-nitro phenyl)-3,4-dihydropyrimidin-2(1H)-one (DHPM-2) has the highest interaction energy, the highest deformation energy, the largest equilibrium coverage of single molecule, and the largest absorption inclination on the Fe(0 0 1) surface comparing with other two molecules. The quantum chemical calculations results, mainly referring to the parameters such as the lower E_{LUMO} , the smaller energy gap ΔE , the largest dipole moment μ , and the Mulliken atomic charge of DHPM-2, also support that DHPM-2 has the higher electron interacting capability with Fe atoms. Consequentially, all of these evidences support an expectation that DHPM-2 has a stronger interaction with Fe atoms in hydrochloric acid aqueous solution, therefore, comparing with the other two organics, the anticipation that DHPM-2 has better inhibition efficiency for mild steel in 1M HCl solution can be concluded. And further, the -NH-CO-NH- group, electronegative oxygen, nitrogen and aromatic ring of these molecules are likely the active centres in the inhibitive adsorption.

ACKNOWLEDGEMENTS

The authors acknowledge the financial support for the research from the material processing key subject of Xi'an Shiyou University (YS32030203) and Technology Creative Foundation of Xi'an Shiyou University (Z08038)

References

1. B. Sanyal, *Prog. Org. Coat.* 9(1981) 165-236.
2. A. Yildırım, M. çtin, *Corros. Sci.* 50(2008) 155-165.
3. D. Zhang, Z. An, Q. Pan, L. Gao, G. Zhou, *Corros. Sci.* 48(2006) 1437-1448.
4. E. M. Sherif, *Mater. Chem. Phys.* 129(2011) 961-967.
5. X. Li, S. Deng, H. Fu, *Corros. Sci.* 53(2011) 3241-3247.
6. E. M. Sherif, *Int. J. Electrochem. Sci.* 7(2012) 4834-4846.
7. K. F. Khaled, M. A. Amin, *Corros. Sci.* 51(2009) 1964-1975.
8. A. Y. Musa, A. A. H. Kadhum, A. B. Mohamad, M. S. Takriff, *Mater. Chem. Phys.* 129(2011) 660-665.
9. K. F. Khaled, *Mater. Chem. Phys.* 124(2010) 760-767.
10. J. Zeng, J. Zhang, X. Gong, *Comput. Theor. Chem.* 963(2011) 110-114.
11. Y. Tang, L. Yao, C. Kong, W. Yang, Y. Chen, *Corros. Sci.* 53(2011) 2046-2049.
12. J. Zhang, G. Qiao, S. Hu, Y. Yan, Z. Ren, L. Yu, *Corros. Sci.* 53(2011) 147-152.
13. J. Zhang, J. Liu, W. Yu, Y. Yan, L. You, L. Liu, *Corros. Sci.* 52(2010) 2059-2065.

14. J. Zhang, W. Yu, L. Yu, Y. Yan, G. Qiao, S. Hu, Y. Ti, *Corros. Sci.* 53(2011) 1331-1336.
15. V. F. Ekpo, P. C. Okafor, U. J. Ekpe, E. E. Ebenso, *Int. J. Electrochem. Sci.* 6(2011) 1045-1057.
16. K. F. Khaled, N. S. Abdel-Shafi, *Int. J. Electrochem. Sci.* 6(2011) 4077-4094.
17. K. F. Khaled, N. S. Abdel-Shafi, N. A. Al-Mobarak, *Int. J. Electrochem. Sci.* 7(2012) 1027-1044.
18. G. C. Rovnyak, K. S. Atwal, A. Hedberg, S. D. Kimball, S. Moreland, J. Z. Gougoutas, B. C. O'Reilly, J. Schwartz, M. F. Malley, *J. Med. Chem.* 35(1992) 3254-3263.
19. L. Xu, L. Zhang, R. Jones, C. Bryant, N. Boddeker, E. Mabery, G. Bahador, J. Watson, J. Clough, M. Arimilli, W. Gillette, D. Colagiovanni, K. Wang, C. Gibbs, C. U. Kim, *Bioorg. Med. Chem. Lett.* 21(2011) 1670-1674.
20. K. Sujatha, P. Shanmugam, P. T. Perumal, D. Muralidharan, M. Rajendran, *Bioorg. Med. Chem. Lett.* 16(2006) 4893-4897.
21. A. S. Paraskar, G. K. Dewkar, A. Sudalai, *Tetrahedron Lett.* 44(2003) 3305-3308.
22. F. Xu, J. Wang, Y. Tian, *Synthetic Communications* 38(2008) 1299-1310.
23. J. Lu, Y. Bai, Z. Wang, B. Yang, H. Ma, *Tetrahedron Lett.* 41(2000) 9075-9078.
24. E. H. Hu, D. R. Sidler, U. Dolling, *J. Org. Chem.* 63(1998) 3454-3457.
25. A. S. Fouda, H. El-Dafrawy, *Int. J. Electrochem. Sci.* 2(2007) 721-733.
26. G. Y. Elewady, *Int. J. Electrochem. Sci.* 3(2008) 1149-1161.
27. N. A. Al-Mobarak, K. F. Khaled, M. N. H. Hamed, K. M. Abdel-Azim, N. S. Abdelshafi, *Arab. J. Chem.* 3(2010) 233-242.
28. N. Caliskan, E. Akbas, *Mater. Chem. Phys.* 126(2011) 983-988.
29. K. Khaled, M. Hamed, K. Abdel-Azim, N. Abdelshafi, *J. Solid State Electr.* 15(2011) 663-673.
30. A. S. Fouda, H. El-Dafrawy, *Int. J. Electrochem. Sci.* 2(2007) 721-733.
31. H. Sun, *J. Phys. Chem. B* 102(1998) 7338-7364.
32. S. L. Li, Y. G. Wang, S. H. Chen, R. Yu, S. B. Lei, H. Y. Ma, D. X. Liu, *Corros. Sci.* 41(1999) 1769-1782.
33. H. Ju, Z. Kai, Y. Li, *Corros. Sci.* 50(2008) 865-871.
34. G. Gece, *Corros. Sci.* 50(2008) 2981-2992.
35. K. F. Khaled, S. A. Fadl-Allah, B. Hammouti, *Mater. Chem. Phys.* 117(2009) 148-155.
36. S. Xia, M. Qiu, L. Yu, F. Liu, H. Zhao, *Corros. Sci.* 50(2008) 2021-2029.
37. W. Shi, C. Ding, J. Yan, X. Han, Z. Lv, W. Lei, M. Xia, F. Wang, *Desalination* 291(2012) 8-14.
38. K. F. Khaled, *Electrochim. Acta* 54(2009) 4345-4352.
39. K. D. Demadis, P. Lykoudis, R. G. Raptis, G. Mezei, *Cryst. Growth Des.* 6(2006) 1064-1067.
40. M. Lashkari, M. R. Arshadi, *Chem. Phys.* 299(2004) 131-137.
41. K. Khaled, *J. Solid State Electr.* 13(2009) 1743-1756.
42. I. Ahamad, R. Prasad, M. A. Quraishi, *Corros. Sci.* 52(2010) 933-942.
43. T. Arslan, F. Kandemirli, E. E. Ebenso, I. Love, H. Alemu, *Corros. Sci.* 51(2009) 35-47.
44. S. Chen, S. Scheiner, T. Kar, U. Adhikari, *Int. J. Electrochem. Sci.* 7(2012) 7128-7139.
45. M. M. Kabanda, L. C. Murulana, E. E. Ebenso, *Int. J. Electrochem. Sci.* 7(2012) 7179-7205.
46. Z. Zhou, R. G. Parr, *J. Am. Chem. Soc.* 112(1990) 5720-5724.
47. K. F. Khaled, *Electrochim. Acta* 48(2003) 2493-2503.
48. A. Popova, M. Christov, T. Deligeorgiev, *Corrosion* 59(2003) 756-764.
49. A. Popova, M. Christov, S. Raicheva, E. Sokolova, *Corros. Sci.* 46(2004) 1333-1350.
50. G. Gece, S. Bilgi, *Corros. Sci.* 51(2009) 1876-1878.